

論文 / 著書情報  
Article / Book Information

Title	Study on Roller-Walker – Adaptation of Characteristics of the propulsion by a Leg Trajectory –
Author	Gen Endo, Shigeo Hirose
Journal/Book name	Proc.IROS2008, , , pp. 1532-1537
発行日 / Issue date	2008, 9
権利情報 / Copyright	(c)2008 IEEE. Personal use of this material is permitted. However, permission to reprint/republish this material for advertising or promotional purposes or for creating new collective works for resale or redistribution to servers or lists, or to reuse any copyrighted component of this work in other works must be obtained from the IEEE.

# Study on Roller-Walker

## – Adaptation of Characteristics of the propulsion by a Leg Trajectory –

Gen Endo and Shigeo Hirose

**Abstract**—Roller-Walker is a leg-wheel hybrid mobile robot using a passive wheel equipped on the tip of each leg. The passive wheel can be transformed into sole mode by rotating ankle roll joints when Roller-Walker walks on rough terrain. This paper describes adaptation of characteristics of the propulsion by a leg trajectory in the case of wheeled locomotion. Firstly, the authors demonstrate that Roller-Walker could achieve high-speed propulsion and slope climbing propulsion by simply changing parameters of the leg trajectory on the hardware experiments. Secondly, an asymptotic parameter tuning method is introduced to perform specified velocity on the different surfaces with different friction. The method is evaluated in numerical simulations. The results suggest that the method allows the Roller-Walker to have a function similar to an automatic transmission of a usual car.

### I. INTRODUCTION

A walking robot which can select discrete foot placements with articulated legs has potential capabilities: 1) it can move adaptively on rugged terrain, 2) it has higher energy efficiency than a wheeled vehicle on soft deformable terrain because it leaves discrete footprints whereas a wheeled vehicle makes continuous furrow which requires larger traction force, 3) it makes holonomic and omnidirectional motion without slip, 4) it can be a stable and movable platform for a manipulator even on rugged terrain when it is not walking. Many walking robots have been developed to move on rugged terrain so far and nowadays some robots edge closer to practical use [1][2].

However, on hard flat terrain, wheeled locomotion is absolutely better than legged locomotion in terms of moving velocity and energy efficiency. Therefore, many research attempt to combine the advantages of these two types of locomotion through leg-wheel hybrid vehicles [3][4][5][6].

In these previous studies, most of the hybrid vehicles equipped with driven wheels, which requires actuators to drive the wheels. Since driven wheels tend to be heavy and bulky, the hybrid vehicles increased the total weight of the robot. We consider that increasing the weight of the robot due to hybridization has a serious defect in walking performance because the walking vehicle is already heavy enough due to many degrees of freedom in the leg mechanisms.

Therefore we have proposed a leg-wheel hybrid vehicle with passive wheels, which are the simplest and lightest wheels [7]. Passive wheels can minimize additional weight for hybridization and do not reduce potential walking performance of the walking robot. Fig. 1 shows overview of

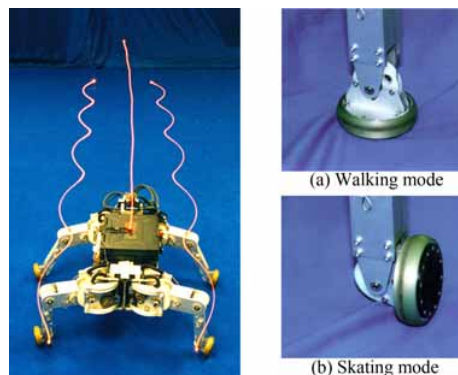


Fig. 1. Roller-Walker: the white lines show trajectories of the frontal leg ends and the body.(left), passive wheel in two modes(right)

the prototype robot of Roller-Walker. Roller-Walker equips with passive wheels on the tip of each leg, and the passive wheel can be transformed into sole mode by rotating ankle roll joint when Roller-Walker walks on rough terrain. Roller-Walker can propel efficiently by means of the same principle of roller-skating on the flat ground. Roller-Walker has distinctive advantages as follows:

- 1) Minimizing additional weight
- 2) Applicable to the previous walking robots
- 3) High power propulsion using legs' actuators
- 4) Potential capability of the terrain adaptation

In particular concerning 4), one of the most interesting property of Roller-Walker is that Roller-Walker can widely change characteristics of the propulsion by modulating the legs' trajectory in wheeled mode. For example, usual driving wheel requires a transmission mechanism to perform both slope climbing locomotion and high speed locomotion. On the contrary, it is expected that Roller-Walker can adapt both different locomotion by simply changing the legs' trajectory.

In our previous work, we derived basic leg trajectories such as straight, circular and rotational propulsion, and we verified in numerical simulations and hardware experiments that Roller-Walker could propel with much higher velocity than walking [7]. However, we did not discuss the relationships between the leg trajectory and propulsive force/velocity characteristics in detail. To the best of our knowledge, there is no detailed report addressing the relationships in the previous studies including biped robots with passive wheels [8][9].

In this paper, we focus on the relation between the leg trajectory and its characteristics of the propulsion for the straight propulsion. Firstly, we do parametric study of

Gen Endo and Shigeo Hirose are with Department of Mechanical and Aerospace Engineering, Tokyo Institute of Technology, #11-60, 2-12-1, Ookayama, Meguro-ku, Tokyo, 152-8552, Japan  
gendo@mes.titech.ac.jp, hirose@mes.titech.ac.jp

the leg trajectories using numerical simulator. The relation between the leg trajectory parameters and physical effects of the propulsion are explained. We then accomplish both high-speed locomotion and slope climbing locomotion on hardware experiments by simply modulating these parameters. Secondly, we discuss adaptation of the leg trajectory parameters in order to perform specified desired velocity. Especially, we introduce an asymptotic parameter adaptation method depending on actual measured velocity and evaluate the method by numerical simulations. The results suggest that the method allows the Roller-Walker to have a function similar to an automatic transmission of a usual car.

## II. SIMULATION MODEL

In this paper, we choose locomotion velocity at steady state as a evaluation criteria because it is one of the most fundamental property of the mobile robots. In this section, we explain a kinematic model and method of numerical analysis for velocity simulations.

There is an infinite of possibilities for the leg trajectory within leg's workspace. To simplify the problem, we assume that; 1) all legs are in support phase, 2) all legs are massless and center of gravity of the robot is located in the middle of the body, 3) left-and-right legs move symmetrical periodic motion. Fig.2 shows a coordinate system for a numerical analysis. The axis of the passive wheel is fixed to the leg at a right angle and its camber angle is also kept at a right angle. We assume a symmetric leg trajectory as follows:

$$d(t) = d_{offset} + d_0(\sin(\omega t + 3\pi/2) + 1), \quad (1)$$

$$\theta(t) = -\theta_0 \sin(\omega t + 3\pi/2 + \phi). \quad (2)$$

$d_0$  and  $\theta_0$  are amplitudes of sinusoidal oscillation in the normal and tangential directions of the passive wheel, respectively.  $\omega$  determines an angular velocity of the oscillations.  $\phi$  is a phase difference between the oscillations in the normal and tangential directions. (Here, we introduce appropriate offsets considering initial posture and leg's workspace of the hardware prototype.) There are four control parameters,  $d_0, \theta_0, \omega, \phi$ , to modulate the leg trajectory in Eqn.(1),(2). An example of the leg trajectory is illustrated in Fig. 2. We assume Coulomb friction at a contact point of the passive wheel on the ground, and thus the resulting tangential force  $F_t(t)$  and normal force  $F_n(t)$  due to the periodic leg motion

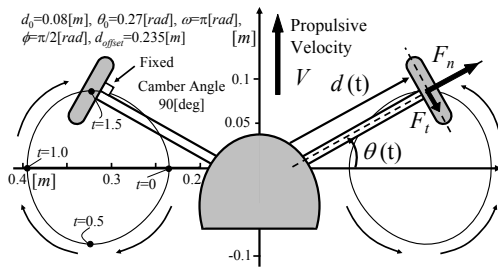


Fig. 2. Simulation model and an example of the leg trajectory(left)

can be expressed as follows:

$$F_t(t) = -\text{sgn}(V \cos \theta(t) + d(t)\dot{\theta}(t)) \cdot \mu_t \cdot mg/4, \quad (3)$$

$$F_n(t) = -\text{sgn}(V \sin \theta(t) + \dot{d}(t)) \cdot \mu_n \cdot mg/4. \quad (4)$$

Here,  $\text{sgn}(\cdot)$  is signum function and  $V$  is propulsive velocity.  $\mu_t, \mu_n$  are Coulomb friction coefficients in the tangential and normal direction, respectively.  $m$  is a total mass of the robot and  $g$  is gravity. The same kinematic model is applied to the hinder legs and we introduce a phase difference of  $\phi_{fr} = 3\pi/2\text{rad}$  between the frontal and hinder legs in order to minimize velocity fluctuation at steady state [7]. Since leg motions are symmetric, the lateral forces are canceled each other out and the sagittal forces remains as a traction force. We obtain activated acceleration of the robot by using the traction force divided by  $m$ . Finally, we calculate propulsive velocity  $V$  by numerical integration of the acceleration. In our study, numerical simulation time step is set to  $10\text{ms}$ .

Additionally, we can derive a necessary condition of propulsion as follows:

$$|F_n(t) \sin \theta(t)| > |F_t(t) \cos \theta(t)|. \quad (5)$$

Here, by substituting Eqn.(3)(4) in above equation, we obtain

$$|\theta(t)| > \tan^{-1}(\mu_t/\mu_n). \quad (6)$$

Eqn.(6) indicates that  $\theta(t)$  to perform propulsion should be larger than the minimum value which is determined by a ratio of friction coefficients of the tangential and normal directions.

We show an example of the result of velocity simulation with a hardware experiment in Fig. 3. Simulated velocity is close to the measured actual velocity with an accuracy of 10% when it reaches steady velocity, suggesting that the velocity simulation has sufficient accuracy for the following parametric study.

## III. LEG TRAJECTORY AND CHARACTERISTIC OF PROPULSION

There are four controllable parameters in Eqn.(1)(2). We discuss the relation between these parameters and intuitive physical effects of the propulsion. The evaluation criteria is averaged velocity  $V$  when the robot performs constant steady velocity. We could search propulsive velocity  $V$  with all combinations of discretized controllable parameters because a numerical simulation can be done for a short time thanks

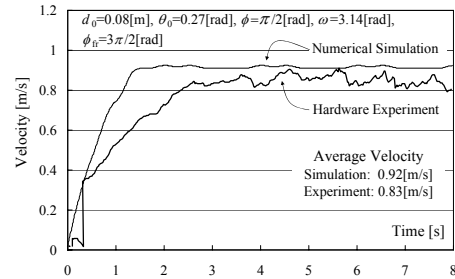


Fig. 3. An example of a numerical simulation

to the simplifying assumptions. The result of the parametric study is summarized as following:

- 1)  $V$  is a monotone increasing function of  $d_0$ .
- 2)  $V$  is proportional to  $\omega$ .
- 3) Unique optimum  $\theta_0$  which gives maximum  $V$  is found.
- 4)  $V$  becomes local maximal value where  $\phi = \pi/2$ .

In the following section, we discuss the relation between  $d_0, \omega, \theta_0$  and  $V$  in detail. (Discussion for  $\phi$  is omitted because of space limitations and we set  $\phi = \pi/2$ .)

#### A. Amplitude of the normal oscillation $d_0$ and angular velocity $\omega$

Roller-Walker generates propulsive movement by utilizing friction differences between the tangential and normal direction. Usually the friction coefficient in the tangential direction  $\mu_t$  is negligible small, traction force is mainly provided with the robot by the friction force in the normal direction  $F_n$ . Therefore, the larger  $d_0$ , amplitude of the oscillation in the normal direction, supplies the larger energy input within one cyclic period. As a consequence, the resultant propulsive velocity  $V$  increases. In terms of supplied energy, the relation between  $\omega$ , angular velocity of the cyclic trajectory, and  $V$  can be explained because supplied energy is proportional to  $\omega$ . Figuratively speaking, we can consider  $d_0$  and  $\omega$  as accelerator of a usual car.

#### B. Amplitude of the tangential oscillation $\theta_0$

It is expected that propulsive velocity  $V$  depends on the friction coefficients  $\mu_n$  and  $\mu_t$ . We also did parametric study of  $V$  where  $\mu_n$  and  $\mu_t$  are parameter, and found that the resultant velocity can be expressed as a function of  $\mu_n/\mu_t$ . Fig.4 shows the relation between  $V$  and  $\theta_0$ , where lines indicate simulated velocity. Fig.4 shows that  $V$  gradually increases when  $\theta_0$  is decreased from larger  $\theta_0$ . However  $V$  rapidly goes down after  $\theta_0$  becomes smaller than the optimum  $\theta_0$  which performs maximum  $V$ . This phenomena can be explained by Eqn.(6) because small  $\theta_0$  does not satisfy necessary condition for propulsion. Additionally, Fig.4 also indicates that  $V$  is not so much depends on  $\mu_n/\mu_t$  where  $\theta_0$  is large value. On the other hand,  $V$  is very much depends on  $\mu_n/\mu_t$  where  $\theta_0$  is small value, and as the larger the  $\mu_n/\mu_t$  value, the larger the  $V$  is generated.

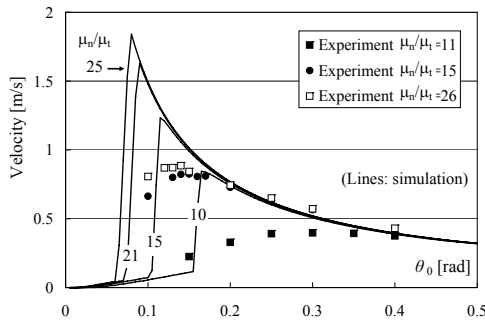


Fig. 4. The relationship between generated velocity and  $\theta_0$  with different friction coefficient ratio ( $d_0 = 0.05m, \phi = \pi/2rad, \phi_{fr} = 3\pi/2, \omega = 3.14rad/s$ )

We conducted numerical simulations applying a backward resistant force to quantitatively evaluate a traction force (Fig.5). It shows that the large  $\theta_0$  allows the robot to propel against the larger resistant force.

These results suggest that  $\theta_0$  determines the ratio of transforming the friction force in the nominal direction  $F_n$  to the traction force in the propulsive direction. In other words,  $\theta_0$  determines a reduction ratio of propulsion. Figuratively speaking, we can consider  $\theta_0$  as transmission of a usual car.

#### C. Hardware Experiment

Firstly, we carried out propulsive velocity experiments using the hardware with various  $\theta_0$ . The experiments were performed on three different surfaces, carpet floor, vinyl floor sheet and rock tile, where  $\mu_n/\mu_t = 11, 15, 26$ , respectively. Measured velocities are plotted in Fig. 4. With large  $\theta_0$ , simulated velocity is similar to measured velocity. However, we can observe large difference with small  $\theta_0$ . The reason would be that simulated velocity accumulates small traction force for long time and finally achieves high locomotion velocity, whereas measured velocity is affected by disturbances mainly because of small bumps on the road surface which prevent the robot from accumulating small traction force. (Additionally, there is large velocity error on the rock tile because  $F_n$  exceeded maximum torque of the leg actuator due to the large friction coefficient  $\mu_n$ . This limitation was not implemented in the numerical simulator.)

Secondly, we implemented manual parameter adjustment system on the hardware robot and carried out velocity experiments on the vinyl floor sheet. An operator could interactively change the parameters of  $(\theta_0, \omega)$ . At the beginning of the experiment, we set  $\theta_0 = 0.3rad, \omega = 0rad/s$  and then gradually increased  $\omega$ . Roller-Walker accelerated very smoothly and its maneuverability was just same as an ordinary car. Moreover, we verified that decreasing  $\theta_0$  from 0.3 to 0.15rad with constant  $\omega$  allowed the robot to smoothly increase propulsive velocity. Maximum propulsive velocity was 2.25m/s where  $d_0 = 0.08m, \theta_0 = 0.15rad, \omega = 1.57rad/s$ , which was very much larger than walking velocity. Additionally we also verified that setting  $\theta_0 = 0.15rad$  could not generate sufficient acceleration force when the propulsive velocity was zero, suggesting that small  $\theta_0$  value can be regarded as small reduction ratio for propulsion.

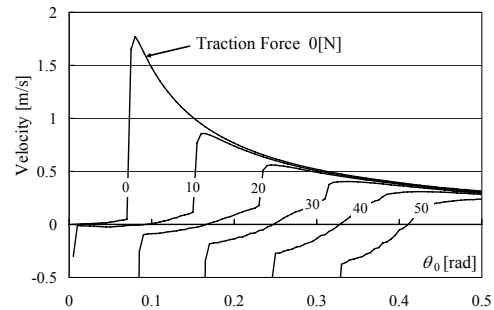


Fig. 5. The relationship between  $\theta_0$  and generated velocity with different traction force ( $d_0 = 0.05m, \phi = \pi/2rad, \phi_{fr} = 3\pi/2, \omega = 3.14rad/s, \mu_n/\mu_t = 25$ )

Thirdly, we investigated a slope climbing experiment on rock tile surface. The inclination of the slope was  $3.0[deg]$  and we set  $\theta_0 = 0.4rad$  which was the maximum value of the hardware prototype robot within leg's workspace. We confirmed that Roller-Walker could climb up the slope with the propulsive velocity of  $0.32m/s$ (Fig.6). This result suggests that large  $\theta_0$  value can be regarded as large reduction ratio for propulsion.

Through the above experiments, we have shown that the propulsive velocity can be controlled by changing  $\omega$  and  $\theta_0$ , and  $\theta_0$  also determines a reduction ratio for propulsion. We have verified a distinctive characteristics of passive wheel propulsion that can be modulated by a leg trajectory.

#### IV. ADAPTATION OF LEG TRAJECTORY PARAMETER

As we mentioned before, Roller-Walker can generate various characteristics of propulsion by changing the leg trajectory parameter. In this section, we introduce an asymptotic parameter adjustment method depending on locomotion environment.

We can observe adaptation of characteristics of propulsion in speed skating, which is based on the same locomotion principle. When a speed skater starts, he or she adjusts skate edge direction to be large angle to the propulsive direction and exhibits a kind of running gait with fast frequent steps. On the other hand, after the skater acquires sufficient high velocity, he or she decreases the angle of the skate edge to the propulsive direction and strongly pushes ice sideways with slow steps. Implementation of such an adaptive function depending on situation and/or environment greatly improves locomotion capability of a Roller-Walker.

In this paper, our objective for a parameter adaptation is to **perform desired velocity**. In the former sections, we investigated the resultant velocity when we set the leg trajectory parameters. In the following section, we reverse the problem. we address parameter settings of the leg trajectory in order to generate given desired velocity. In particular, we introduce an asymptotic parameter adaptation method based on an error between measured velocity and desired velocity. We show that introduced method works appropriately even with friction coefficient change in numerical simulations.

In the following section, we set  $d_0 = 0.08m$ ,  $\phi = \pi/2rad$  to simplify the problem, and thus we assume propulsive velocity  $V = f(\theta_0, \omega)$ . We derive parameters of  $(\theta_0, \omega)$  to perform desired velocity  $V_d$ . (Note that  $V$  denotes actual measured velocity of the robot in the following section. )



Fig. 6. Achievement of slope climbing propulsion ( $\theta_0 = 0.4rad$ ,  $\omega = 2.88rad/s$ ,  $V = 0.32m/s$ )

#### A. Empirical formula of propulsive velocity

We empirically search simulated  $V$  with different  $(\theta_0, \omega)$  sets considering leg's workspace and actuator power of the hardware robot (Fig.7). We use friction coefficients of vinyl floor sheet,  $\mu_n = 0.417$ ,  $\mu_t = 0.026$ . As we mentioned in the Section II, we can assume  $V \propto \omega$ . And we obtain empirical formula of propulsive velocity by fitting the relation between  $V$  and  $\theta_0$  using a third order polynomial function,

$$V(\theta_0, \omega) = f(\theta_0, \omega) = \omega \cdot g(\theta_0) \quad (7)$$

$$= \omega \sum_{k=0}^3 a_k \theta_0^k \quad (8)$$

where  $a_0 = 1.256$ ,  $a_1 = -7.349$ ,  $a_2 = 18.556$ ,  $a_3 = -16.947$  and  $f(*)$ ,  $g(*)$  denote functions. The lines in Fig.7 show sufficient accuracy of the approximation by Eqn.(8).

If we can solve Eqn.(8) for  $(\theta_0, \omega)$ , we obtain required parameters  $(\theta_0, \omega)$  to perform given  $V_d$ . However, supposing a usual car, there is an infinite of possibilities for transmission ratios and engine revolutions that achieve the same velocity. Thus, we can not solve a unique solution. Therefore we introduce parameter adaptation method based on physical considerations in the following section.

#### B. $\theta_0$ adaptation law

When Roller-Walker achieves given desired velocity, small  $\theta_0$  provides the robot with small  $\omega$ . Generally speaking, a leg mechanism of a walking machine is usually designed to equip with actuators with a high reduction ratio to produce sufficient force to sustain body's weight. Thus, small  $\omega$  is preferable for a walking robot. However as we demonstrated in Section III.C, small  $\theta_0$  could not produce large traction force and the propulsion of the robot became sensitive to disturbance force. On the other hand, large  $\theta_0$  is suitable for acceleration phase and slope climbing which require large propulsive force, and it is robust against disturbance force. However large  $\theta_0$  requires large  $\omega$  when the robot performs high-speed locomotion and sometimes it is not feasible for the hardware. Therefore we introduce  $\theta_0$  adaptation law that generates large  $\theta_0$  value in acceleration/deceleration phase to supply sufficient traction force. And it also generates small  $\theta_0$  value when the robot achieves desired velocity. The adaptation is driven by velocity error, which is the difference between actual measured velocity and desired velocity. Here,

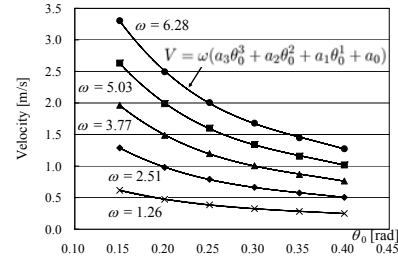


Fig. 7. Simulated propulsive velocity with parameter  $\theta_0$  and  $\omega$  on the vinyl floor

$\theta_0^{target}$ ,  $\theta_0^{max}$ ,  $\theta_0^{min}$  are target, minimum and maximum value of  $\theta_0$ , respectively. We design  $\theta_0^{target}$  as follows;

$$\theta_0^{target} = \begin{cases} \theta_0^{max} & |V/V_d - 1| > tol, \\ \theta_0^{min} & otherwise, \end{cases} \quad (9)$$

where  $tol$  is a tolerance of velocity control. If velocity error is larger than  $tol$ , it indicates that the robot requires acceleration/deceleration. Thus, we design  $\theta_0^{target} = \theta_0^{max}$ . And if velocity error is less than  $tol$ , we set  $\theta_0^{target} = \theta_0^{min}$  in order to decrease  $\omega$ . To ensure smooth continuous change of  $\theta_0$ , we introduce the following dynamics;

$$\dot{\theta}_0 = -k_{\theta_0}(\theta_0 - \theta_0^{target}), \quad (10)$$

$$\theta_0 \leftarrow \theta_0 + \dot{\theta}_0 \cdot \Delta t, \quad (11)$$

where  $k_{\theta_0}$  is a feedback gain and  $\Delta t$  is a simulation time step.

### C. $\omega$ adaptation law

With given  $V_d$  and  $\theta_0$ , we can solve Eqn.(7) for  $\omega_d$ .

$$\omega_d = V_d / g(\theta_0), \quad (12)$$

where  $\omega_d$  denotes desired  $\omega$  value. Similar to  $\theta_0$  change, we introduce a feedback gain  $k_{\omega_d}$  and following dynamics,

$$\dot{\omega} = -k_{\omega_d}(\omega - \omega_d), \quad (13)$$

$$\omega \leftarrow \omega + \dot{\omega} \cdot \Delta t. \quad (14)$$

However the empirical formula Eqn.(8) is acquired by numerical simulations on a particular surface, vinyl floor sheet. It can be used as a rough estimated target but it is not sufficient to achieve desired velocity when the robot on a different surface with different friction coefficient and/or a sloped surface. Therefore we introduce an additional feedback term based on actual measured velocity  $V$  as follows;

$$\dot{\omega} = -k_{\omega_d}(\omega - \omega_d) - k_v(V - V_d), \quad (15)$$

where  $k_v$  is a feedback gain for the velocity error. As a matter of convenience in the following discussion, we call Eqn.(13) and Eqn.(15) as “Nominal  $\omega$  adaptation” and “Actual  $\omega$  adaptation”, respectively.

## V. NUMERICAL EVALUATION

In this section, we evaluate the introduced adaptation method using numerical simulations. Firstly, we verified  $\omega$  adaptation to perform specified desired velocity. Fig.8 shows the result of velocity control with nominal  $\omega$  adaptation on vinyl floor sheet, where  $\theta_0 = 0.15rad$ , initial values are set as  $\omega_0 = 3.14rad/s$ ,  $V = 0.0m/s$ .  $k_{\omega_d}$  is set as 10.0 in order to converge to nominal  $\omega_d$  within 1sec. The velocities after sufficient course of time reached desired velocity  $V_d$  very well.

However as we mentioned, nominal  $\omega$  adaptation is effective only in the case that a road surface is the exactly same as the derivation of Eqn.(8). The black thin line in Fig. 9 indicates the propulsive velocity with nominal  $\omega$  adaptation on a carpet floor,  $\mu_n = 0.61$ ,  $\mu_t = 0.057$ . While desired velocity is  $V_d = 0.5m/s$ , achieved actual averaged velocity

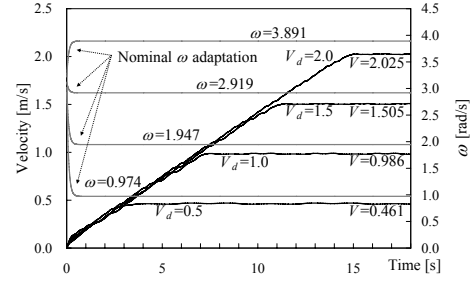


Fig. 8. Velocity control by nominal  $\omega$  adaptation (Eqn.(13)) (Black lines are  $V$  and gray lines are  $\omega$ )

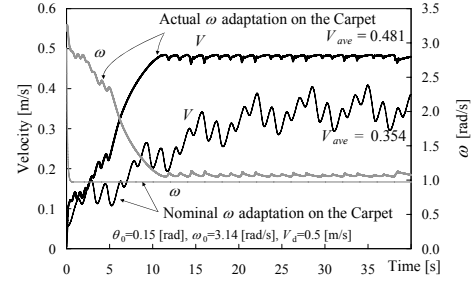


Fig. 9. Improvement of velocity control accuracy introducing actual  $\omega$  adaptation (Eqn.(15)) on the carpet

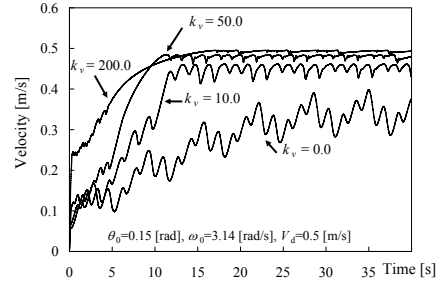


Fig. 10. Velocity convergence of actual  $\omega$  adaptation with various  $k_v$

after sufficient course of time  $V_{ave}$  is  $0.354m/s$ . There is a large difference between  $V_d$  and  $V_{ave}$ .

Then we evaluated actual  $\omega$  adaptation, where  $k_v = 50.0$ . The black bold line in Fig. 9 shows the propulsive velocity with actual  $\omega$  adaptation.  $V_{ave}$  is improved from 0.354 to  $0.481m/s$  and achieved velocity is sufficiently close to  $V_d = 0.5m/s$ . This result suggests that asymptotic parameter adaptation based on the actual velocity error is effective against change of friction coefficient.

To investigate the stability with actual  $\omega$  adaptation, we carried out velocity simulations with different  $k_v$ . Ideally speaking, a formal proof of the stability is preferable. However, the propulsive velocity is generated by the frictional force and it is hard to construct a realistic formula. Thus, we investigated convergence of the velocity using the numerical simulator.  $k_v$  was modulated in the range of 0 - 200 where the other simulation conditions were the same as Fig. 9. Fig. 10 indicates that actual  $\omega$  adaptation is stable in the broad range of  $k_v$ . The reason would be that the frictional force works as an inherent stable feedback. Because the frictional force always occurs in order to minimize a slip of the passive wheel and the force instantaneously changes

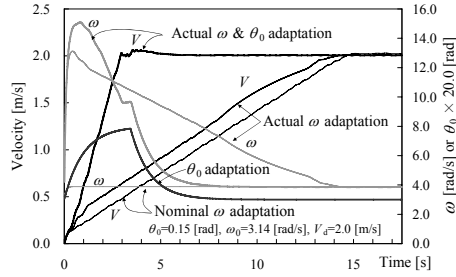


Fig. 11. Improvement of acceleration with  $\theta_0$  adaptation

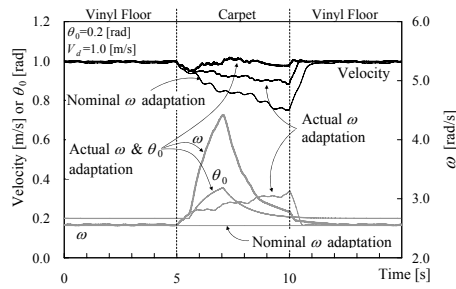


Fig. 12. Robust velocity control with actual  $\omega$  and  $\theta_0$  adaptation on different surfaces (Upper three lines: Velocity, Lower 4 lines:  $\omega$  and  $\theta_0$ )

direction opposing the slip (Eqn.(3)(4)).

Secondly, we investigated the effect of  $\theta_0$  adaptation when the robot accelerate from initial velocity of zero to desired velocity of  $V_d = 2.0 \text{ m/s}$  on the vinyl floor sheet (Fig.11). There is no difference after 15sec in terms of  $V$  in the steady state. However, acceleration performances are very different depending on the parameter adaptations. With only nominal  $\omega$  adaptation, where  $k_{\omega_d} = 10.0$ ,  $\omega$  reached constant value at 0.4sec and  $V$  gradually increased. It took 15sec to reach  $V_d$ . With actual  $\omega$  adaptation, where  $k_{\omega_d} = 10.0$ ,  $k_v = 50.0$ ,  $\omega$  largely increase at the starting phase, but  $V$  did not increase so much. Because small  $\theta_0$  could not generate sufficient traction force. With actual  $\omega$  adaptation and  $\theta_0$  adaptation, where  $k_{\omega_d} = 10.0$ ,  $k_v = 50.0$ ,  $k_{\theta_0} = 1.0$ ,  $\theta_0$  rapidly increased for initial 3sec and  $V$  reached  $V_d$  five times faster than without introducing  $\theta_0$  adaptation. And after achieving  $V_d$ ,  $\theta_0$  and  $\omega$  automatically decreased while keeping the same propulsive velocity  $V$ . This result suggests that introduced  $\theta_0$  adaptation is quite effective for the fast acceleration propulsion.

Finally, we conducted propulsive simulations on different surfaces (Fig.12). We changed friction coefficients from the vinyl floor sheet to the carpet floor for 5.0 – 10.0sec. With nominal  $\omega$  adaptation, the robot decreased  $V$  on the carpet area. With actual  $\omega$  adaptation, the degree of velocity decrease was less but not sufficient. On the contrary, with introducing  $\theta_0$  adaptation,  $\theta_0$  and  $\omega$  rapidly increased on the carpet area and successfully kept constant  $V_d$ . These adaptation is qualitatively equivalent to the “kick down shift control” of a usual automatic transmission car.

These results suggest that introducing  $\theta_0, \omega$  adaptation allows the robot to keep  $V_d$  robust regardless of friction coefficient change.

## VI. CONCLUSION

In this paper, we focus on the relation between characteristics of the propulsion and leg trajectory for passive wheeled locomotion of a Roller-Walker. Firstly, we conducted parametric search to understand the relation between leg trajectory parameters and physical effects of propulsion. Then, we pointed out the parameters, which are qualitatively equivalent to gas pedal or shift lever of a usual car. Secondly, we demonstrated that high-speed locomotion and slope climbing locomotion were possible by adjusting these parameters with hardware experimentations. Thirdly, we introduced an asymptotic parameter adaptation method to achieve desired velocity using actual measured velocity. Finally, we evaluated the introduced method by numerical simulations. The results suggest that introducing  $\theta_0, \omega$  adaptation is effective to accomplish desired velocity.

As mentioned, the introduced method is an example of trajectory adaptation and not a unique solution. However, we demonstrated that adjusting leg trajectory could provide the Roller-Walker with similar control scheme as a usual automatic transmission of a car.

We plan to carry out hardware experimentation. Robust sensing of the propulsive velocity is one of the key issues for a successful implementation. We expect that averaging dead reckoning measurements of four passive wheels with rotary encoders performs robust measurement.

Furthermore, we plan to analyze energy efficiency in wheeled locomotion. To evaluate energy efficiency, estimation of actual disturbance and consideration of hardware limitations are very important. Incorporating these effects on the numerical simulator will increase accuracy of simulations. Trajectory optimization in terms of energy efficiency forms an important part of our future work.

## REFERENCES

- [1] T. Doi, R. Hodoshima, Y. Fukuda, S. Hirose, J. Mori, and T. Okamoto, “Development of a quadruped walking robot to work on steep slopes, titan XI (walking motion with compensation for compliance),” in *Proc. of Int. Conf. on Intelligent Robots and Systems*, 2005, pp. 3413–3418.
- [2] [http://www.gearlive.com/index.php/news/article/plustechs\\_walking\\_forest\\_machine\\_03150832/](http://www.gearlive.com/index.php/news/article/plustechs_walking_forest_machine_03150832/).
- [3] Y. Dai, E. Nakano, T. Takahashi, and H. Ookubo, “Motion control of leg-wheel robot for an unexplored rough terrain environment,” in *Proc. of 7th Int. Conf. on Advanced Robotics*, vol. 2, 1995, pp. 911–916.
- [4] H. Adachi, N. Koyachi, T. Arai, A. Shimizu, and Y. Nogami, “Mechanism and control of a leg-wheel hybrid mobile robot,” in *Proc. of Int. Conf. Intelligent Robots and Systems*, 1999, pp. 1792–1797.
- [5] S. J. Ylonen and A. J. Halme, “Workpartner - centaur like service robot,” in *Proc. of Int. Conf. Intelligent Robots and Systems*, 2002, pp. 727–732.
- [6] C. Grand, F. BenAmar, F. Plumet, and P. Bidaud, “Decoupled control of posture and trajectory of the hybrid wheel-legged robot hylos,” in *Proc. of Int. Conf. Robotics and Automation*, 2004, pp. 5111–5116.
- [7] G. Endo and S. Hirose, “Study on roller-walker (multi-mode steering control and self-contained locomotion),” in *Proc. of Int. Conf. on Robotics and Automation*, 2000, pp. 2808–2817.
- [8] M. Kumagai and K. Tamada, “Roller-walk of a biped robot using a truck with variable curvature,” in *Proc. of ROBOMECH’07*, 2007, pp. 2A1–J02(in Japanese).
- [9] K. Hashimoto, Y. Sugahara, T. Hosobata, Y. Mikuriya, H. Sunazuka, M. Kawase, H. Lim, and A. Takanishi, “Sliding motion of biped walking robots mounted on passive wheels – 1st report: Realization of swizzle motion by inline skates –,” in *Proc. of ROBOMECH’07*, 2007, pp. 1A1–E11(in Japanese).